Journal of Alloys and Compounds 503 (2010) L26–L30

Contents lists available at ScienceDirect

Journal of Alloys and Compounds

journal homepage: www.elsevier.com/locate/jallcom

Letter

Refinement of hypereutectic Al–Si alloy by a new Al–Zr–P master alloy

Min Zuo, Kun Jiang, Xiangfa Liu*

Key Laboratory for Liquid-Solid Structural Evolution and Processing of Materials, Ministry of Education, Shandong University, Jinan 250061, Shandong, PR China

ARTICLE INFO

Article history:
Received 9 March 2010
Received in revised form 3 May 2010
Accepted 3 May 2010
Available online 10 May 2010

Keywords:
Al–Si alloy
ZrP
AlP
Microstructure
Phase transformation

ABSTRACT

In this article, a novel Al–6Zr–2P master alloy with ZrP particles was successfully synthesized. Field-emission scanning electron microscope (FESEM) observation on the phases extracted from the master alloy showed flaky $ZrAl_3$ phase adheres to the ZrP particles, indicating ZrP phase would precipitate firstly in the solidification process and then the $ZrAl_3$ phase attaches to the pre-formed ZrP particles and grows. The reason for the excellent refining performance of Al–6Zr–2P master alloy was that Si clusters could promote the transformation of ZrP to AlP and subsequently AlP acts as the heterogeneous nucleation sites of primary Si phase.

1. Introduction

Considerable efforts have been devoted to the development of hypereutectic Al–Si alloys, due to their excellent wear and corrosion resistance, lower density, higher thermal stability and outstanding mechanical properties [1–3]. However, primary Si exhibits rather irregular morphologies such as coarse platelet and polygon, which have detrimental effects on the mechanical properties of hypereutectic Al–Si alloys. Therefore, these Si precipitations must be effectively refined. Many researches have focused on the improvement of refiners to meet the requirements of environmental protection and industry applications. Phosphorus is well accepted as one of the most effective refiners of primary Si at the addition level of a few hundred parts per million (ppm), which can be traced back to the patent by Sterner and Rainer in 1933 [4]. It is well established that P is generally used due to the AlP particles formed in the melt, which is zinc–blende structure with lattice parameter $a = 0.545$ nm [5]. According to the literatures [6–8], Si can nucleate heterogeneously on a substrate of AlP with a cube–cube orientation relationship and solidify to form a faceted Si particle due to the very similar parameters with AlP. At present, phosphorus is added into the alloy melt mainly in the form of master alloys due to their simplicity, such as Cu–P, Al–Cu–P, Al–Fe–P and Al–Si–P master alloys [9–14].

During the past decades, borides, carbides and nitrides of transition metals have been widely studied. Only a few investigations of the phosphides have been done, although some phosphides have some good physical and chemical properties. For example, ZrP are such transition metal phosphides, which are of much interest in view of its high chemical and thermodynamic stability even at elevated temperatures [15–21]. ZrP shows relatively strong corrosion resistance of acid solutions, for example Hydrochloride. Meanwhile, the decomposition temperature of ZrP is up to 1000 K [15,19–20] and ZrP in the NaCl structure has been observed to be superconducting with transition temperatures up to 5 K [21].

In chemistry, a phosphide is a compound of phosphorus with a less electronegative element or elements, and many transition metals can react with phosphorus to form various stoichiometry phosphides. However, this is not necessarily the case in Al-based alloy. In this study, a new type of Al-based master alloy – ternary Al–6Zr–2P master alloy has been successfully developed in which P takes the form of ZrP particles. Meanwhile, the refining performance of new master alloy on the hypereutectic Al–Si alloys was investigated and refinement mechanism was also discussed.

2. Experimental procedures

The commercial pure Zr and binary Al–3.5P master alloy were used to prepare the novel Al–6Zr–2P master alloy in high-temperature melting furnace (all composition quoted in this work are in wt.% unless otherwise stated). The binary Al–3.5P master alloy was firstly melted, and then pure Zr was added into the melt. After holding at 1450–1600 °C for about 20 min, the melt was poured to obtain an ingot. The base alloy used in refining experiment was hypereutectic A390 alloy which was prepared with commercial purity Al (99.85%), Si (99.5%) and other commercial purity elements using a medium frequency induction furnace. The refining treatment of A390 alloys was as follows: after the A390 alloy was melted at 780 °C, the melt was degassed with C_2Cl_6 for 15 min; subsequently, the refining treatment was carried out with the addition of 1.5 wt.% Al–6Zr–2P master alloy. After different holding time, the melt was poured into a permanent mould (70 mm × 35 mm × 20 mm) pre-

* Corresponding author. Tel.: +86 531 88392006; fax: +86 531 88395414.
E-mail address: xfliu@sdu.edu.cn (X. Liu).

0925-8388/$ – see front matter © 2010 Elsevier B.V. All rights reserved.
doi:10.1016/j.jallcom.2010.05.017

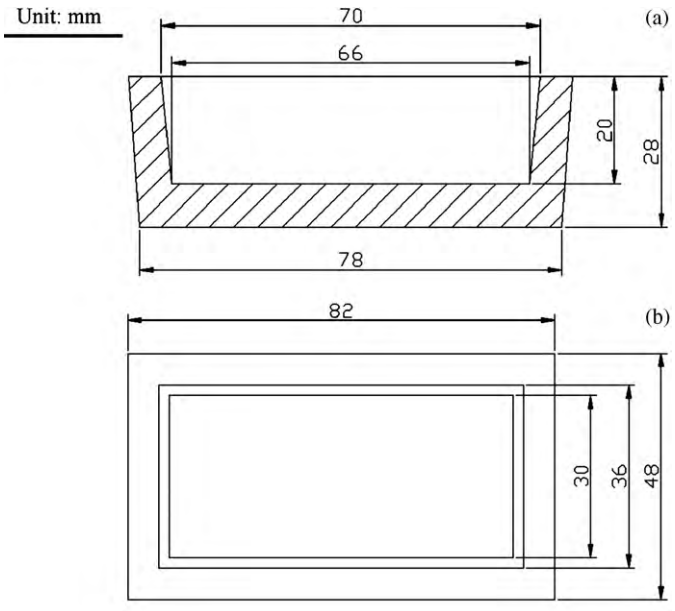

Fig. 1. Pattern dimensions of the pouring mould used in grain refining tests: (a) sectional view and (b) vertical view.

heated to 150 °C. The pouring mold used in the refining treatments is illustrated in Fig. 1.

Metallographic specimens of A390 alloys were cut from the intermediate portion of the casting samples, then mechanically ground and polished through standard routines. The mean size of primary Si was measured from photomicrographs, averaging at least 10 areas of metallographic specimens, and in each area about 10 primary Si particles were chosen. In order to further investigate the microstructure of Al–6Zr–2P master alloy, the compound particles were obtained by using the extraction technology. The specific operating procedures of the extraction treatment were as follows: first, the specimens of Al–6Zr–2P master alloy were etched with certain concentration of hydrochloric acid solution; after the alloys were dissolved, the particles were collected using centrifugal extractor and rinsed with distilled water and ethanol for several times and then desiccated. Subsequently, the phase compositions were identified by X-ray diffraction (XRD) and the microstructure analysis was carried out by FESEM equipped with energy dispersive X-ray spectrometer (EDS).

3. Results and discussion

The XRD pattern of Al–6Zr–2P master alloy is shown in Fig. 2(a). According to the XRD pattern, the Al–6Zr–2P master alloy is composed of α-Al, $ZrAl_3$ and ZrP phases. Irani and Gingerich reported that when ZrP is heated above 1425 °C, it would undergo a hexagonal (h) to cubic (c) phase transition [16]. Under the present conditions in fabrication process, ZrP exhibits only the cubic form, which can be demonstrated by the XRD pattern mentioned above. The diffraction line exhibits peaks at 29.3°, 34.0° and 48.8° corresponding respectively to the (1 1 1), (2 0 0) and (2 2 0) reflections of face-centered cubic (fcc) ZrP. The reason for the only cubic ZrP formation appears most likely that the high-temperature cubic phases of ZrP are nucleated first and then quenched rapidly before the cubic phase can convert to the low-temperature hexagonal phase [16].

Typical FESEM photomicrographs of the Al–6Zr–2P master alloy have been illustrated in Fig. 2(b) and (c). As revealed in Fig. 2(b), there are two phases in the grayish α-Al matrix. According to EDS analysis, the coarse flaky-shaped phase can be identified as $ZrAl_3$ with an average composition of $ZrAl_{2.81}$. Meanwhile, the regular blocky phase with about 10 μm in size is a compound containing elements of Zr and P, and can be deduced to be cubic ZrP. Fig. 2(c) shows the representative FESEM image of the extracted ZrP grain, which presents the cubic three-dimensional morphologies clearly. As shown in Fig. 2(d), the flakes adhering to ZrP particles are the $ZrAl_3$ phase. Therefore, it can be deduced that the ZrP phase would precipitate firstly in the solidification process of Al–6Zr–2P system,

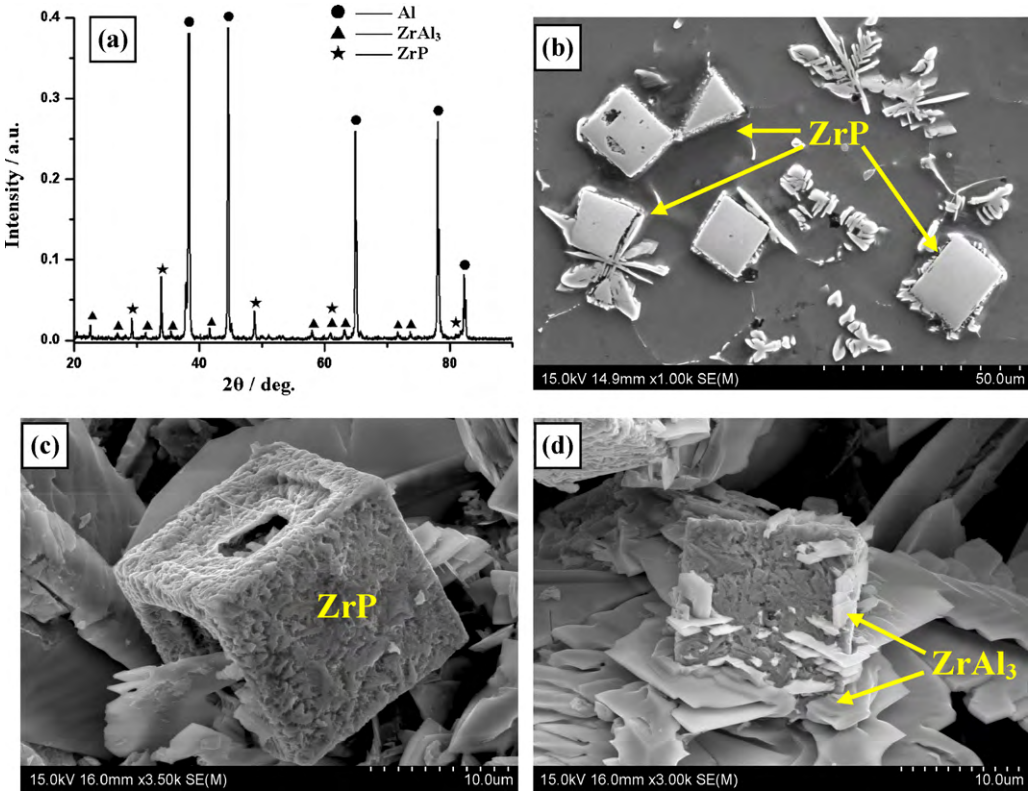

Fig. 2. XRD patterns and FESEM micrographs of ternary Al–6Zr–2P master alloy: (a) XRD patterns; (b) microstructure; (c and d) the images of phases extracted from the master alloy system.

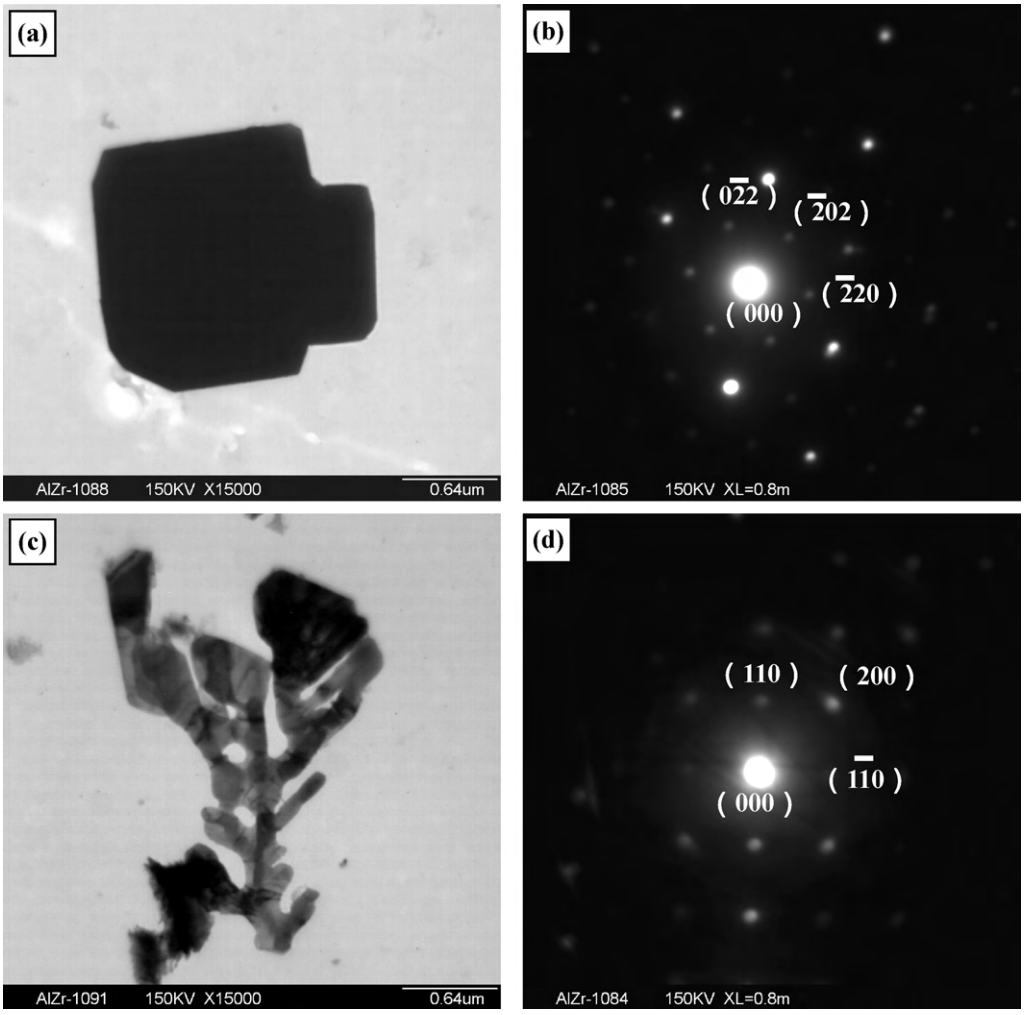

Fig. 3. TEM analysis for the grains extracted from the Al–6Zr–2P master alloy: (a and b) the morphology and the corresponding SAED pattern of ZrP in zone axis of [1 1 1]; (c and d) the morphology and the corresponding SAED pattern of $ZrAl_3$ in zone axis of [0 0 1].

and then the $ZrAl_3$ phase would separate on the pre-formed ZrP particles and subsequently grow.

Fig. 3 shows the TEM analysis for the ZrP and $ZrAl_3$ grains extracted from the Al–6Zr–2P master alloy. The corresponding selected-area electron diffraction (SAED) patterns of ZrP [1 1 1] zone axis and $ZrAl_3$ [0 0 1] zone axis are shown in Fig. 3(b) and (d) respectively.

Refining tests were carried out to quantify the refining performance of the new Al–6Zr–2P master alloy. Fig. 4 shows the typical microstructures of A390 alloys unrefined and refined by 1.5 wt.% Al–6Zr–2P master alloy. As illustrated in Fig. 4(a), the primary Si in unrefined A390 alloys presents irregular morphologies with an average size of 95.5 μm. As evident in Fig. 4(b), A390 alloys have shown fast grain refinement response to the addition of the new master alloy, with average size of primary Si significantly decreasing to 18.3 μm even holding for only 15 min. At the holding time of 90 min, the average size of primary Si is about 17.7 μm (standard deviation: 1.77 μm), indicating that the new developed Al–6Zr–2P master alloy is a high efficient refiner with a good fading resistance.

The reason for the excellent refining performance of Al–6Zr–2P master alloy with pre-formed ZrP particles is a question that needs to be addressed. Some elements might have the influence on the ZrP phase and promote the transformation from ZrP to AlP which is an ideal heterogeneous nucleation of primary Si [6–8]. The hypereutectic A390 alloy used in the refining experiment mainly consist of 17.5% Si, 4.5% Cu, 0.5% Mg and balance Al. Among these elements, Si as the major alloying element was taken into account to investigate its influence on the ZrP particles due to its relatively active reaction with Zr. Subsequently, different amounts of Si were introduced into the Al–Zr–P system, and the corresponding XRD patterns were shown in Fig. 5(a). Quite different from that of ternary Al–6Zr–2P alloy, the diffraction reflections of $ZrAl_3$ are not observed on the XRD patterns of quaternary Al–Si–Zr–P systems, meanwhile the diffraction intensity of ZrP phase remarkably weakens with the increase of Si content. Furthermore, XRD patterns reveal the presence of two Zr-rich phases: ZrSi (orthorhombic, Cmcm, $a = 0.376$ nm, $b = 0.992$ nm, $c = 0.375$ nm) and $ZrSi_2$ (orthorhombic, Cmcm, $a = 0.372$ nm, $b = 1.461$ nm, $c = 0.367$ nm), and the intensity of diffraction peaks of ZrSi and $ZrSi_2$ phases increases as Si content rises.

What is particularly worth mentioning is that, there is certain limitation in XRD analysis method to verify the AlP particles in the presence of Si phases due to the fact that they have the identical diffraction peaks. Therefore, further investigations were carried out to confirm the presence of AlP particles and FESEM micrograph of the Al–18Si–6Zr–2P alloys is illustrated in Fig. 5(b). It can be seen that there were two phases in the α-Al matrix besides Si phases. Among them, the light-colored phase was a kind of Zr-rich intermetallic compound with an average composition of 34.25 at.% Zr, 57.90 at.% Si and balance Al, and can be interpreted as the phase $ZrSi_2$. In addition, an oxygen-rich compound was found to be enveloped with the primary Si. It has been demonstrated that

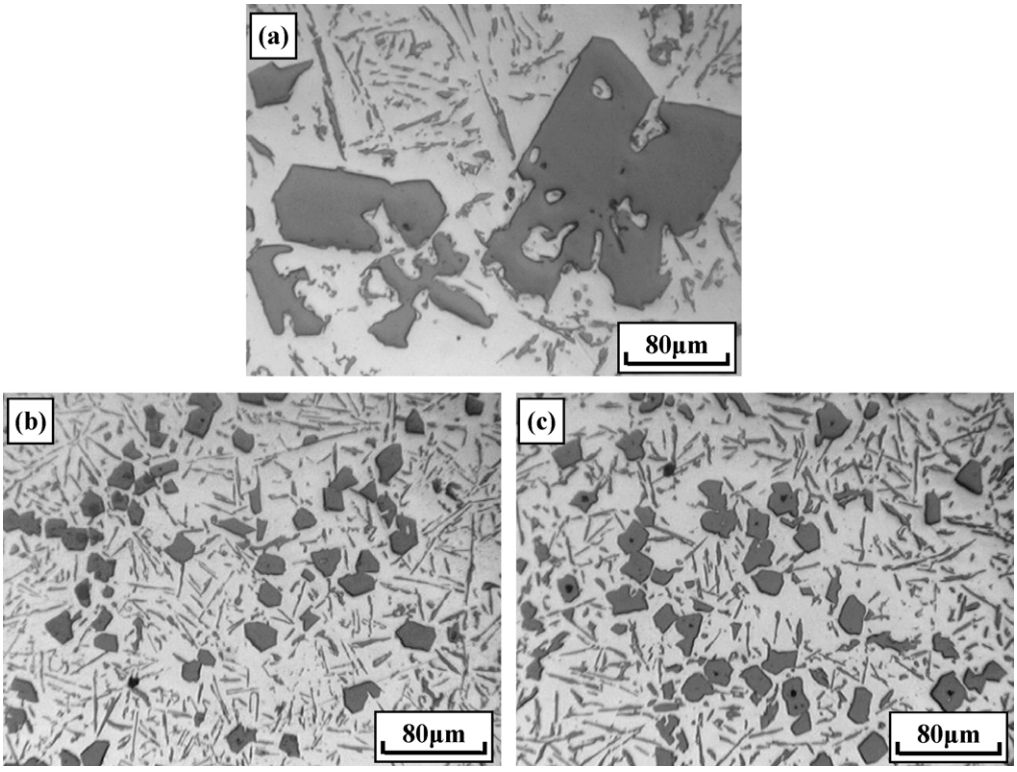

Fig. 4. Typical microstructures of A390 alloy before and after the addition of Al–6Zr–2P master alloy: (a) unrefined; (b and c) refined by 1.5 wt.% Al–6Zr–2P master alloy at 780 °C with 15 min and 90 min, respectively.

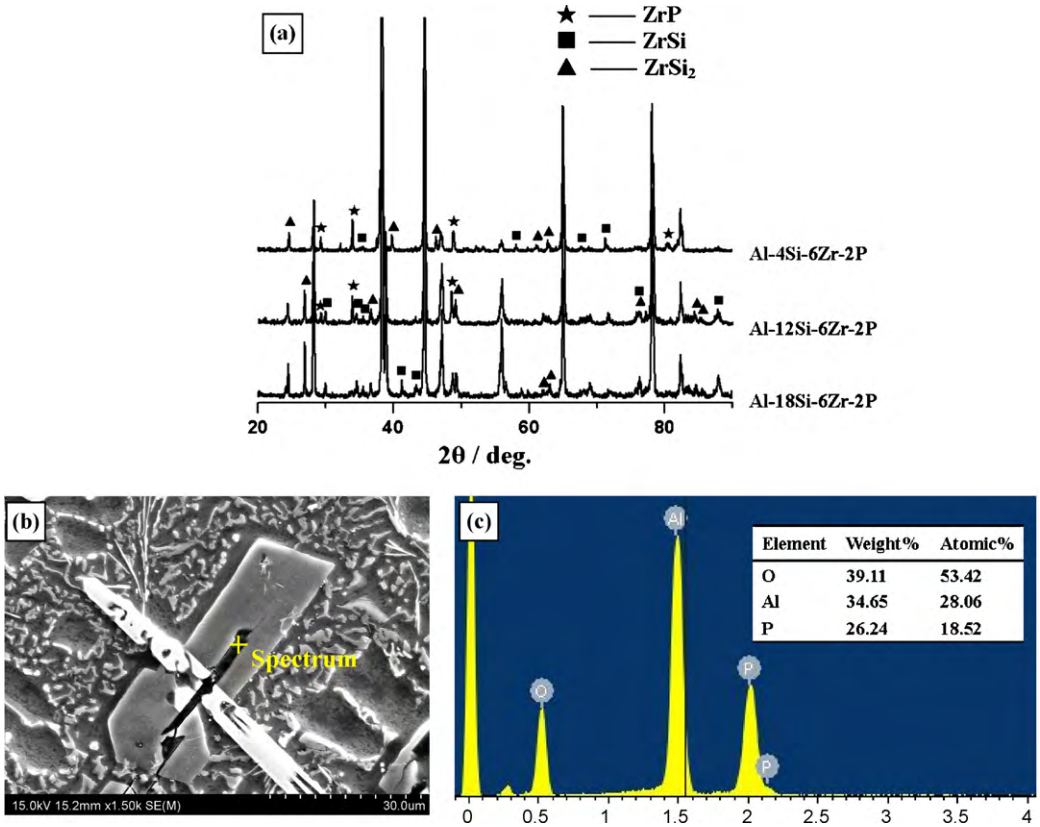

Fig. 5. XRD patterns and corresponding FESEM images for the Al–Si–Zr–P systems: (a) XRD patterns; (b) FESEM image of Al–18Si–6Zr–2P alloy; (c) EDS spectra of corresponding dot in (b). Unmarked diffraction peaks in (a) belong to Al, Si and AlP phases.

the distribution of oxygen is likely to correspond with the phosphorus distribution, which appears to be due to a rapid-oxidation event of the P-rich particle [22]. Therefore, it is reasonable to deduce that the black intermetallic compounds are the AlP particles, which is just the evidence used to support the transformation from ZrP to AlP.Combined with the results of XRD, the influence of Si doping into the Al–6Zr–2P system could be described as the following reactions.

$$ZrAl_3 + Si \rightarrow ZrSi/ZrSi_2 + Al \quad (1)$$

$$ZrP + Si \rightarrow ZrSi/ZrSi_2 + P \quad (2)$$

$$Al + P \rightarrow AlP \quad (3)$$

This explanation is feasible to deduce the reactions among the elements Si, Zr and P when the Al–6Zr–2P master alloy was added into the melt. In the A390 alloy melt, the driving force of the reactions listed above would be much greater than that of Al–18Si–6Zr–2P alloy due to the relative higher Si concentration. When added into the A390 melt, the ZrP would react with Si clusters to release P via diffusion. Consequently, P would precipitate in the form of AlP particles which act as the heterogeneous nucleation of primary Si in the solidification process.

4. Conclusions

In summary, the introduced Zr element optimizes the Al-based master alloys containing P in which P takes the form of AlP, and a novel Al–6Zr–2P master alloy with stable ZrP particles has been successfully prepared. The ZrP particles are characterized by a higher chemical and thermodynamic stability compared with AlP particles. It is proposed that the Si atoms in the melt could promote the transition of ZrP to AlP, which would be the reason for the excellent refining performance of the developed Al–6Zr–2P master alloy.

Acknowledgements

This work was supported by a grant from National Science Fund for Distinguished Young Scholars of China (No. 50625101), and Key Project of Science and Technology Research of Ministry of Education of China (No. 106103).

References

[1] J. Li, M. Elmadagli, V.Y. Gertsman, J. Lo, A.T. Alpas, Mater. Sci. Eng. A 421 (2006) 317–327.
[2] M.M. Haque, A. Sharif, J. Mater. Process. Technol. 118 (2001) 69–73.
[3] V.C. Srivastava, R.K. Mandal, S.N. Ojha, Mater. Sci. Eng. A 383 (2004) 14–20.
[4] R. Sterner, C. Rainer, US Patent 1940922, 26 December 1933.
[5] A. Addamiano, J. Am. Chem. Soc. 82 (1960) 1537–1540.
[6] C.R. Ho, B. Cantor, Acta Metall. Mater. 43 (1995) 3231–3246.
[7] B. Cantor, Mater. Sci. Eng. A 226–228 (1997) 151–156.
[8] Q. Ma, Acta Mater. 55 (2007) 943–953.
[9] F.C. Robles Hernandez, J.H. Sokolowski, J. Alloy Compd. 426 (2006) 205–212.
[10] H.H. Zhang, H.L. Duan, G.J. Shao, L.P. Xu, Rare Met. 27 (2008) 59–63.
[11] D.Y. Maeng, J.H. Lee, C.W. Won, S.S. Cho, B.S. Chun, J. Mater. Process. Technol. 105 (2000) 196–203.
[12] M. Faraji, I. Todd, H. Jones, J. Mater. Sci. 36 (2001) 2667–2672.
[13] M. Zuo, X.F. Liu, Q.Q. Sun, K. Jiang, J. Mater. Process. Technol. 209 (2009) 5504–5508.
[14] Q. Zhang, X.F. Liu, H.S. Dai, J. Alloy Compd. 480 (2009) 376–381.
[15] K.A. Gingerich, Nature 200 (1963) 877–1877.
[16] K.S. Irani, K.A. Gingerich, J. Phys. Chem. Solids 24 (1963) 1153–1158.
[17] L.Y. Chen, M.X. Huang, Y.L. Gu, L. Shi, Z.H. Yang, Y.T. Qian, Mater. Lett. 58 (2004) 3337–3339.
[18] R.F. Jarvis, R.M. Jacubinas, R.B. Kaner, Inorg. Chem. 39 (2000) 3243–3246.
[19] R.L. Ripley, J. Less-Common Met. 4 (1962) 481–584.
[20] S. Motojima, T. Wakamatsu, K. Sugiyama, J. Less-Common Met. 82 (1981) 1–404.
[21] A.R. Moodenbaugh, D.C. Johnston, R. Viswanathan, Mater. Res. Bull. 9 (1974) 1589–1692.
[22] Y.H. Cho, H.C. Lee, K.H. Oh, A.K. Dahle, Metall. Mater. Trans. A 39 (2008) 2435–2448.